Manuscript

http://dx.doi.org/10.1039/b209976d

Schmedt auf der Günne, J. Eckert, H. Léaustic, A.; Babonneau, F. Vacancy ordering and host-guest interactions in $CdPS_3$ intercalates: Results from multidimensional solid state NMR. *Phys. Chem. Chem. Phys.* **2003**, *5*, 1306–1313.

Vacancy ordering and host-guest interactions in $CdPS_3$ intercalates: Results from multidimensional solid state NMR

Jörn Schmedt auf der Günne[a,*], Hellmut Eckert[a],

Anne Léaustic[b], Florence Babonneau[c]

[a]Institut für Physikalische Chemie, Westfälische Wilhelms-Universität,

Schlossplatz 4/7, 48149 Münster, Germany

[b]Laboratoire de Chimie Inorganique, Université Paris-Sud Bât 420,

91405 Orsay Cedex, France

[c]Chimie de la Matière Condensée, Université Paris 6 - T54 -E5 4

place Jussieu, 75252 Paris Cedex 05, France

Abstract

Cadmiumhexathiohypodiphosphate ($CdPS_3$) intercalates with potassium and N,N'-dimethylviologen cations have been studied by complementary one- and two-dimensional solid state NMR experiments. The intercalation process results in vacancies in the Cd sublattice, whose detailed distribution is sensitively reflected in both the ^{31}P and the ^{113}Cd spectra of the host material. Advanced 2-D ^{31}P double quantum and spin echo NMR techniques are used to further investigate the connectivity patterns of the ^{31}P atoms represented by the peaks observed. Simple chemical shift considerations strongly indicate that the vacancy distribution is primarily controlled by electrostatic repulsion effects. Thus a model is developed for the local vacancy arrangement that links structural motifs with stoichiometry and the NMR results.

In the case of the methylviologen intercalate NMR allows to study the interaction between the organic guest molecule and the host material. Owing to strong Coulombic interactions, one positively charged end of the molecule is pinned at a minimum distance to the negatively charged Cd vacancy in the layer on the NMR time scale, while the other end is orientationally disordered relative to the layers. This arrangement provides an excellent fit to the experimental intensity distributions in the one- and two-dimensional ^{31}P MAS NMR spectra.

*corresponding author; current address: Institut für Anorganische Chemie; Universität Bonn; Gerhard-Domagk-Straße 1; 53121 Bonn; Germany; Telephone: 0049-228-733333; Email Address: gunnej@uni-bonn.de

Introduction

MPS_3 layered materials (M = transition metal), namely metal hexathiohypodiphosphates, have attracted much attention over the last 20 years because of their ability to form intercalation compounds with various inorganic and organic species [1]. During this process M^{2+} ions are removed from the layers, leaving vacancies behind. The local charge of these vacancies is compensated by ionic guest species A^{n+}, which are inserted into the interlayer space, according to the following reaction scheme:

$$MPS_3 + 2\frac{x}{n} A^{n+} \rightarrow M_{1-x}A_{2\frac{x}{n}}PS_3 + x\, M^{2+}$$

Insertion results in a dramatic modification of the physical properties, which has led to various applications as nonlinear optical materials [2, 3], as magnetic materials [4, 5], as catalysts and as cathode materials in battery applications [6,7]. Different synthetic approaches [6,8,9] combining a variety of host [10] and guest molecules [2, 3, 11–13] have been developed.

The structural consequences of intercalation have been widely studied by powder diffraction methods. Besides measuring changes in the interlayer distance [8], more complex issues have been addressed, such as the question of whether the product maintains some type of order, be it ordering of the vacancies or of the inserted molecules. Ordering of guest molecules has been shown to occur in several cases [3,14,15]. To find proof for vacancy ordering is much more difficult since vacancies can be traced spectroscopically only by indirect

evidence. Nevertheless it was possible to find hints for vacancy ordering in the magnetic measurements of an iron cadmium thiophosphate [16] and in XRD-measurements of intercalated $MnPS_3$ [15]. Mößbauer spectroscopy was also used to probe ordered and disordered vacancy distributions [16, 17]. Being an element-selective, inherently quantitative method with excellent local resolution power, high resolution solid-state NMR has shown great promise as a structural tool of characterizing disorder in solid state materials [18]. Recently it was shown that the ^{31}P chemical shift is a sensitive probe of local order in lamellar thiophosphates [19]. Based on this result NMR should be able to detect site inequivalencies created by the intercalation process. Furthermore, sophisticated dipolar methods are available to identify connectivity and spatial proximity between phosphorus sites [20–23].

In this contribution we exploit the potential of such techniques to examine the vacancy distribution in lamellar metal hexathiohypodiphosphates. As model systems we have chosen the potassium and methylviologen (structural formula see figure 9) intercalates of $CdPS_3$,

$$Cd^{2+}_{1-x}A^{n+}_{2\frac{x}{n}}(P_2S^{4-}_6)_{0.5} \quad A = \text{Methylviologen}^{2+}, K^+ \tag{1}$$

They can readily be obtained by wet chemistry and have been well characterized by structural techniques [8, 9, 12, 16, 17]. We will present multinuclear solid state NMR data on these materials and discuss them in relation to potential vacancy distribution scenarios.

Experimental

Sample Preparation and Characterization

Samples were prepared by topotactic ion exchange according to the following equation, where the intercalation coefficient x is a measure for the degree of intercalation.

$$CdPS_3 + 2\frac{x}{n}A^{n+} + yH_2O \rightarrow Cd^{2+}_{1-x}A^{n+}_{2\frac{x}{n}}(P_2S_6^{4-})_{0.5} \cdot yH_2O + xCd^{2+} \quad (2)$$

$$CdPS_3 + xMV^{2+} + yH_2O \rightarrow Cd_{1-x}MV_xPS_3 \cdot yH_2O + xCd^{2+} \quad (3)$$

$$CdPS_3 + 2xK^{+} + yH_2O \rightarrow Cd_{1-x}K_{2x}PS_3 \cdot yH_2O + xCd^{2+} \quad (4)$$

The pure $CdPS_3$ host compound was synthesized by the procedures already described in a previous publication [24] by heating stoichiometric amounts of the elements with 2% excess of sulphur in an evacuated quartz ampule at 680 °C for two weeks. The potassium intercalate $Cd_{1-x}K_{2x}PS_3(H_2O)$ was obtained by ion exchange. For this purpose 200 mg of $CdPS_3$ were stirred with 10 ml of 0.1 M EDTA as complexing agent, 10 ml of 0.5 M KCl and a 0.25 M K_2CO_3/$KHCO_3$ buffer solution at room temperature. After 12 h the solution was renewed and stirring continued for another 12 h.

The synthesis of methylviologen intercalate was obtained by treating pure

$CdPS_3$ (200 mg) with a solution of methylviologendichloride (300 mg) in methanol (3 ml) for one day at 60 °C.

Characterization of the compounds and their intercalates was carried out by elemental analysis and X-ray powder diffraction. X-ray diffraction patterns of the powders were recorded in reflection mode on a Siemens diffractometer with a CuK_α radiation source ($\lambda = 1.5405$ Å). The diffraction patterns in transmission mode (figure 2) were recorded on an INEL CPS 120 diffractometer using 0.3 mm capillaries. Calibration was done with $Na_2Ca_3Al_2F_{14}$ (cubic parameter: a = 10.257 Å) [25]. Elemental analysis was carried out by the CNRS analytical service (France).

Cadmium hexathiohypodiphosphate intercalated with methylviologen cations (abbreviated as MV^{2+}) and potassium cations will in this article be referred to as methylviologen intercalate and potassium intercalate, respectively.

Solid State NMR

The ^{31}P NMR experiments were carried out on a Bruker DSX500, the ^{15}N, ^{13}C and ^{113}Cd experiments on a Bruker MSL300 NMR spectrometer equipped with commercial 4 mm and 7 mm MAS-NMR probes; the magnetic field strengths were 11.7 T and 7.05 T respectively. The quality factor of the probe that was used for the ^{31}P experiments, was lowered to 100 by adding a 150 kΩ resistor in parallel to the coil. Samples were rotated within zirconia spinners. By means of appropriate Teflon spacers, the sample was confined to the middle $1/3$ of the rotor volume. A commercially available pneumatic

control unit was used to limit MAS frequency variations to a 2 Hz interval for the duration of the experiment. Chemical shifts are externally referenced to 85% phosphoric acid for ^{31}P, to solid NH_4NO_3 (10% ^{15}N enriched sample; $\delta_{iso}(NO_3^-) = -4.6\,\text{ppm}$ compared to CH_3NO_2 ($\delta_{iso} = 0\,\text{ppm}$)) for ^{15}N, to TMS for ^{13}C and to 1 M $Cd(NO_3)_2$ aqueous solution for ^{113}Cd NMR. 2-D spin echo spectroscopy experiments were carried out, using MAS at a spinning speed of 15 kHz and rotor-synchronized incrementation in the t_1 domain (266 experiments). Eight transients with the appropriate phase cycling were used [26]. The excitation time in the double-quantum experiments (figure 1) consists of a continuous-wave block of two rotor periods length, with 14 different phase entries as previously detailed [27]. This block was repeated eight times to an overall length of 533 μs excitation time. Phase cycling used during the excitation period and during the acquisition were set to select the coherence pathways $\Delta p = 0 \rightarrow \pm 2 \rightarrow 0 \rightarrow -1$. All data were acquired with a four-step phase cycle and a z-filter delay of 30 ms before the read pulse, using the States method for obtaining pure absorption 2-D double-quantum spectra. The rf field strength was optimized for each sample by adjusting the amplifier power on a 2π pulse of fixed length, while the rf field strength used for the final read pulse was determined independently. A 2 μs phase preset time for the digital phase shifter was chosen. The evolution time t_1 in these 2-D experiments was rotor-synchronized in all experiments. A pulse train of 30 $\pi/2$-pulses with a spacing of 30 ms (saturation comb) was used in all experiments to suppress unwanted phase coherences due to an insufficiently short chosen

repetition rate. Typical experimental conditions were: recycle delay 25 s, 256 t_1 increments. ^{113}Cd MAS NMR spectra were obtained under the following conditions: MAS-spinning frequency 10 kHz, pulse length 4 μs corresponding to a flip angle of 90°, 300 s repetition delay and $600-800$ transients. ^{15}N CP MAS NMR spectra were obtained under the following conditions: MAS-spinning frequency 5 kHz, nutation frequency for ^{15}N 42 kHz, contact time 5 ms, recycle delay 10 s, 17000 transients. Cross polarization conditions were optimized on NH_4NO_3. ^{13}C CP MAS NMR spectra were obtained under the following conditions: MAS-spinning frequency 5 kHz, nutation frequency for ^{13}C 42 kHz, contact time $0.1-10$ ms, recycle delay 10 s, 1200 transients. Cross polarization conditions were optimized on adamantane.

Results

The host material, crystalline $CdPS_3$, has only one crystallographic site for both the cadmium and phosphorus atoms [10]. The ^{31}P and ^{113}Cd NMR spectra thus only show single resonances at 103.6 ppm (figure 3) and 480 ppm (figure 4) respectively. Elemental analysis carried out on this material, which is also the educt for the intercalates shown below, shows a small excess of sulphur, corresponding to the composition $CdPS_{3.11}$(S:40.15%, P : 12.48%).

The elemental analysis of a series of potassium and methylviologen intercalates proves that the composition is batch dependent. The compositions vary around an average of $Cd_{0.77\pm0.02}K_{0.45\pm0.04}PS_{3.0\pm0.1}(H_2O)$ and

$Cd_{0.85\pm0.02}MV_{0.15\pm0.02}PS_{3.0\pm0.1}$.

From a series of batches two were chosen for further investigation by solid state NMR. Chemical analysis led to the following formulae:

$Cd_{0.78}K_{0.44}PS_{3.12}(H_2O)_{1.05}$ (P:11.80%, S:38.21%,K:6.56%,H:0.81%)

$Cd_{0.84}MV_{0.16}PS_{3.05}(H_2O)_{0.13}$ (P:11.70%,S:36.96%,C:8.39%,H:0.93%,N:1.65%)

Formulae were derived setting the phosphorus fraction to one and assuming the cation insertion would be charge balanced by the cadmium cation removal.

X-ray diffraction patterns of the potassium and methylviologen intercalates recorded in a reflection geometry display only sharp 00*l* peaks due to the preferential orientation. The basal spacing is 9.46 Å for the potassium intercalate and 9.89 Å for the methylviologen intercalate, while it is only 6.55 Å in the host $CdPS_3$ material. The patterns have also been recorded in a transmission geometry to detect all the *hkl* peaks (figure 2). A comparison with the X-ray pattern of $CdPS_3$ [10] shows common features indicating that the main structural motifs of the host structure are maintained in the intercalation compounds. One can notice also the presence of additional peaks of weaker intensities.

In the ^{31}P NMR spectra of the potassium intercalate up to five resonances are observed (figure 3). The center resonance at $\delta = 99.2$ ppm appears within a few hours while the sample is rotating inside the magnet and dominates

the spectrum in aged samples. The structural changes associated with this aging effect could be related to a migration of potassium guest ions into the Cd^{2+} vacancies, but this effect will not be subject to further investigation here. In a freshly prepared sample this peak has negligible intensity compared to the other resonances. 2D ^{31}P NMR MAS spin echo spectroscopy allows to resolve and assign the other observed four peaks to two chemically distinct hexathiohypodiphosphate groups in the structure (figure 5). The peaks at $\delta = 102.3$ ppm and 102.0 ppm belong to chemically inequivalent P atoms of the same $P_2S_6^{4-}$-group, the splitting yields $^1J(^{31}P -^{31} P) \approx 75$ Hz. The peaks at $\delta = 97.4$ ppm and 96.3 ppm belong to chemically inequivalent P atoms of a second $P_2S_6^{4-}$-group, the splitting yields $^1J(^{31}P -^{31} P) \approx 86$ Hz in this case. This assignment is supported by ^{31}P MAS 2D double quantum spectroscopy (figure 6). Each of the $P_2S_6^{4-}$-groups gives rise to its appropriate double quantum signals. The intensity ratio of the two pairs of peaks is $1.00/0.96 \approx 1$. The ^{113}Cd NMR MAS spectra show one resonance at 439 ppm (figure 4 B).

In the ^{31}P NMR spectra of the methylviologen intercalate only one resonance containing some fine structure can be observed (figure 3). The signal spreads over an interval from 100.4 ppm to 102.5 ppm. The ^{31}P NMR MAS double quantum spectrum reveals more details (figure 7). In particular, a characteristic triangular pattern is observed, indicating the presence of ^{31}P spin pairs, in which one P site resonates near 100.4 ppm, whereas the chemical shift of the other site varies over a wider range. Figure 7 includes four cross-sections of the DQ-spectra highlighting the spectra of different ^{31}P spin

pairs. Each of these resonances is split by indirect spin-spin coupling (shoulders on the signals in the cross sections). In the ^{113}Cd NMR MAS spectrum two broad overlapping peaks at 439 ppm and 470 ppm can be observed. The intensity ratio of the two peaks is $\frac{\text{int.}_{439\,\text{ppm}}}{\text{int.}_{470\,\text{ppm}}} \approx 60:40$. A second spectrum at a lower spinning speed shows a significantly higher chemical shift anisotropy for the resonance at $\delta = 439\,\text{ppm}$ (data not shown).

The ^{15}N CP MAS NMR spectrum recorded on the methylviologen intercalate (figure 8) shows three resonances at -170.0, -174.6 and $-177.6\,\text{ppm}$, representing three N environments. The ^{13}C CP MAS NMR spectra (figure 9) present peaks around 50 ppm (N-CH_3), 130 ppm ($C_{2,2'}$) and 146 ppm ($C_{1,1',3}$). With increasing contact time, three peaks due to the methyl carbon at 49.0, 51.6 and 53.3 ppm can be distinguished that exhibit different cross polarization dynamics. A similar behaviour can also be noticed for the peaks at 124.4, 127.5 and 130.2 ppm.

Discussion

The ^{31}P and ^{113}Cd NMR data bear important information regarding the vacancy distribution in these intercalation compounds. To help the graphical representation of different vacancy scenarios, we introduce a two dimensional picture based on the cadmium position in one layer (figure 10). This hexagonal honeycomb-type presentation of the cadmium sites uses the assumption that adjacent layers have insignificant influence on each others' vacancy or-

dering and that the main structural motifs of the host structure are maintained in the intercalation compound, in agreement with XRD results. Both of these assumptions are well accepted in the literature. Considering the distribution of the Cd-vacancies created by the intercalation process, we assume further that cadmium vacancies will not be direct neighbours, since the Coulomb repulsion should penalize this arrangement both from a kinetic and a thermodynamic point of view. As a direct consequence of this assumption the maximum number of Cd vacancies near a given $P_2S_6^{4-}$ group is three. Thus four environments, corresponding to zero, one, two and three distinct neighbouring vacancies can occur in principle. Likewise, each Cd^{2+} ion can in principle be situated next to zero, one, two, or three vacancies. The average number of vacancies directly situated next to a phosphorus $\overline{\#Vac.^{P_2S_6}}$ or cadmium $\overline{\#Vac.^{Cd}}$ atom (based on the chemical composition according to formula 1), is given by:

$$\overline{\#Vac.^{Cd}} = 3\frac{x}{1-x} \tag{5}$$

$$\overline{\#Vac.^{P_2S_6}} = 6x \tag{6}$$

These formulae can be derived easily by taking into account that the stoichiometry at different intercalation levels x has to be obeyed. The intercalation level x is known from chemical analysis. In case of the two intercalates chosen for this study we get:

	$\overline{\#Vac.^{P_2S_6}}$	$\overline{\#Vac.^{Cd}}$
Methylviologen Intercalate $x = 0.16 \pm 0.01$	0.96 ± 0.06	0.57 ± 0.03
Potassium Intercalate $x = 0.22 \pm 0.01$	1.32 ± 0.06	0.85 ± 0.03

The observation of distinct ^{31}P and ^{113}Cd peaks indicates that the vacancies are localized on the NMR timescale. Therefore NMR spectroscopy is able to provide the fractions of phosphorus and cadmium species with no, a single, two and three directly neighboured vacancies p_0, p_1, p_2 and p_3, provided these give rise to peaks with different chemical shifts. These fractions can be related to the average number of vacancies.

$$\overline{\#Vac.^{P_2S_6/Cd}} = 0\,p_0 + 1\,p_1 + 2\,p_2 + 3\,p_3 \tag{7}$$

Thus, key to the analysis of the NMR-spectra is the interpretation of the observed chemical shifts. One striking detail of all the ^{31}P and ^{113}Cd resonances of the intercalated materials is that they are more shielded than those of the pure host. In fact this is not unexpected since the negatively charged holes in the structure convey a higher electronic density to both the cadmium and phosphorus atoms. The effect arises most likely from modifications of both the diamagnetic and the paramagnetic terms in the Ramsey equation for chemical shifts [28]: The negatively charged vacancy in the neighborhood of a P or a Cd atom not only increases the diamagnetic shielding term, but also reduces the paramagnetic deshielding effect created by p- or d-electron imbalance in the valence shell [29]. We view this effect in close analogy to the well- known ^{1}H and ^{13}C chemical shift trends in organic molecules: electron-pushing lig-

ands cause low-frequency shifts, while electron withdrawing ligands result in high-frequency shifts. The applicability of this general concept to ^{31}P chemical shifts is also supported by trends observed experimentally in various alkali phosphates and thiophosphates, revealing an increase in ^{31}P chemical shift with increasing cation electronegativity (table 1). Based on these considerations we assume that the ^{31}P and ^{113}Cd chemical shifts are dominantly affected by the number of vacancies directly situated around a phosphorus or cadmium atom, more vacancies resulting in stronger low-frequency shifts. This hypothesis is also in agreement with the interpretation of previous Mößbauer chemical shifts in the Fe-analogues of $CdPS_3$ in [17], and as well with the observation that in the methylviologen intercalate the ^{113}Cd resonance with the lower ppm value has a bigger chemical shift anisotropy. This is expected since the neighbouring vacancy will deform the local Cd environment, creating a more asymmetric electron distribution near the nucleus.

The Potassium Intercalate

The observation of only two P_2S_6 groups of equal intensity for the potassium intercalate clearly indicates that the vacancy distribution in this compound is non-random. The averaged number of vacancies around phosphorus $\overline{\#Vac.^{P_2S_6}} = 1.32 \pm 0.06$ and cadmium $\overline{\#Vac.^{Cd}} = 0.85 \pm 0.03$ are close to the idealized values of $\overline{\#Vac.^{P_2S_6}} = 1.5$ and $\overline{\#Vac.^{Cd}} = 1.0$, on which we will base our discussion. The only two possible sets of population distributions which have only two nonzero but equal fractions and satisfy the conditions

imposed by equations 6 and 7 are: $\{p_0^{P_2S_6} = 0,\ p_1^{P_2S_6} = 0.5,\ p_2^{P_2S_6} = 0.5,\ p_3^{P_2S_6} = 0\}$ and $\{p_0^{P_2S_6} = 0.5,\ p_1^{P_2S_6} = 0,\ p_2^{P_2S_6} = 0,\ p_3^{P_2S_6} = 0.5\}$. The latter is chemically not sensible, thus the vacancy distribution can be visualized with the hexagonal layer representation as in figure 10. The chemical shift of 102.2 ppm is assigned to the $P_2S_6^{4-}$-groups near one vacancy, while the chemical shift of 96.8 ppm is assigned to the $P_2S_6^{4-}$-groups adjacent to two vacancies. Just taking into account the ^{31}P NMR data many other arrangements leading to the same set of fractions would be possible. In this connection the ^{113}Cd resonance imposes one further experimental restriction however. The observation of a single resonance at 439 ppm is consistent with a unique Cd^{2+} environment, having one neighbouring vacancy as displayed in figure 10.

The Methylviologen Intercalate

In case of the methylviologen intercalate the spread of the ^{31}P NMR chemical shifts observed is narrower than that expected if several P_2S_6 groups were present having different numbers of directly neighboured vacancies (compare figure 3). Instead, the ^{31}P chemical shift region indicates that in the case of the methylviologen intercalate only one type of P_2S_6-group with a single neighbouring vacancy is present, i.e. $p_1^{P_2S_6} = 1$ (corresponding to an intercalation coefficient of $x = \frac{1}{6}$) in agreement with the average number of vacancies $\overline{\#Vac.^{P_2S_6}} = 0.96 \pm 0.06$. The corresponding vacancy distribution can be visualized as in figure 11. The hatching of the hexagons indicates that three

hexagons with one vacancy can be seen as the building unit of the layer. Since there is no possibility to construct a layer from this basic unit with more than one vacancy directly neighboured to a cadmium, the fractions p_2^{Cd} and p_3^{Cd} have to be zero. It follows that 57% of the cadmium have one and 43% of the cadmium have no neighbouring vacancy. This compares to an experimental intensity ratio of $60/40$ in the ^{113}Cd-spectrum. The peak at 470 ppm is thus assigned to a cadmium with no neighbouring vacancy, and the peak at 439 ppm is assigned to one with one vacancy. This is in agreement with the chemical shift of pure $CdPS_3$ at 480 ppm and also with the assignment done in the potassium intercalate.

An interesting detail left to explain is the peculiar shape of the ^{31}P double-quantum peak of the methylviologen intercalate. Since the spread in chemical shift is small, it is reasonable to explain the shape by the interaction of the P_2S_6 groups with the intercalated organic guest molecule in the free space between the layers. The XRD results strongly suggest that the methylviologen entities lie with the plane of the aromatic rings parallel to the layer of the host material, thus it is instructive to compare the length scales of the host with the guest molecule. In the methylviologen cation MV^{2+} the charge is localized at the nitrogen atoms, which have a distance of 700 pm relative to each other. This distance is too small to allow a correlation of the two positive charges in the methylviologen with two vacancies in the same layer. Following the arguments presented above on the interpretation of chemical shifts, the neighbourhood of an electron withdrawing positive charge to a sulphur atom

in the layer will result in a deshielding of the phosphorus bonded to this sulphur atom. This effect will be smaller and opposite to the effect of the direct neighbourhood of a negatively charged vacancy. Again the magnitude of this effect will depend on the distance between positively charged nitrogens and three sulphur atoms. In this connection we can define three types of interaction spots (figure 12). Type **A** is characterized by three sulphur atoms which are bonded to the same phosphorus atom, type **B** by a spot which is confined by three sulphur atoms which belong to two different P_2S_6-groups and in type **C** the sulphur atoms originate from three different P_2S_6-groups. Based on the above considerations, we expect the ^{31}P nuclei to become increasingly deshielded in the direction **C**→**B**→**A**, reflecting the increasing proximity of the positive charge. Type **C** corresponds to the energetically most favorable configuration, where the negatively charged vacancy and the positively charged N atom of the guest species are at minimum distance. In terms of the strength of the Coulomb interaction between a vacancy and the methylviologen there are two possible cases. Either the interaction is weak compared to the thermal energy (case I), then there will be no correlation between the vacancy and the positive charge of a nitrogen, producing a statistical ^{31}P shift distribution. Alternatively, if the interaction is strong (case II), then there will be a correlation and this should change the chemical shift distribution.

A crude estimate for a statistical ^{31}P chemical shift distribution (case I) may be derived by counting the number of triangles below the positive charges of the two nitrogen atoms. Statistically type **A**, **B** and **C** occur with probabil-

ities of 16.7%, 50% and 33.3%, respectively. In case II the positive charge at one end of the MV^{2+}ion is fixed at an interaction spot of type **C** while the charge situated at the other end is disordered and distributed over one of the triangles in a circle with a radius of the nitrogen nitrogen distance of 700 pm. Thus one gets a total probability of a positive charge interacting with a type **C** spot of $(100\% + 37.5\%)/2 \approx 69\%$ (see table 2) as the sum of the interactions of both nitrogen atoms. In a similar fashion[1] numbers for the intensities of the various 2D cross sections can be predicted for both scenarios (figure 13). As shown in figure 13 only scenario II reproduces both the distribution in the 1D as well as the peculiar triangular peak shape in the double quantum spectrum seen in the experimental data with the highest intensity in the **CC**-autocorrelation signal. Thus we can understand the cross sections in figure 7 to represent three different kinds of P_2S_6-groups namely **CC**, **CB** and **CA**, respectively. Note that P_2S_6-groups of types **AB**, **AB** and **BB** are not detected. This result confirms that the Coulomb interaction between the cationic guest species and the anionic vacancy has a significant influence on the location of the MV^{2+} cation within the interlayer space.

Further evidence for this model comes from the ^{13}C and ^{15}N NMR spectra. The ^{13}C NMR peaks which originate from the methyl carbon are split into three (see figure 9) and the same is true for the ^{15}N NMR results (see figure 8). Each of the three peaks can again be identified with one of the interaction spots **A**, **B** and **C**. A more detailed analysis is not possible here because

[1]The two dimensional double-quantum spectrum can be derived with a random distribution of the phosphorus atoms on either side of a P_2S_6-layer, e.g the intensity for the autocorrelation signal AA is $0.69^2 \approx 48\%$.

of the non-quantitative nature of CP-MAS.

It remains to be said that the XRD powder patterns recorded on the potassium and the methylviologen intercalate show extra peaks and modified intensities compared to the XRD pattern of pure $CdPS_3$ suggesting the appearance of a superstructure, in accordance with the proposed models.

Conclusions

From the analysis of the data presented here it may be concluded that the vacancy distribution in these $CdPS_3$ intercalates is determined mainly by the Coulomb repulsion between two vacancies. Thus it is possible to determine the vacancy distribution simply from the stoichiometry of the compound. Coulomb interactions also dominate the location of the methylviologen guest species relative to the layers of the host material, resulting in a minimum distance between the positively charged N atom and the Cd vacancy in the layer. The results of this study illustrate the power of complementary solid state NMR techniques to resolve subtle structural issues in layered intercalation compounds. Based on these results ^{31}P NMR may be used to measure the intercalation coefficient in systems which follow the proposed model.

Acknowledgments

J. S. a. d. G. would like to thank the Fonds der Chemischen Industrie for a personal fellowship. Financial support for this work from DFG grant Ec168-1 is most gratefully acknowledged. The authors would like to thank Dr. N. Lequeux (ESPCI, Paris, France) for the X-ray diffraction patterns recorded in transmission mode.

References

[1] R. Brec, *Solid State Ionics*, 1986, **22**, 3–30.

[2] I. Lagadic, P. G. Lacroix, and R. Clément, *Chem. Mater.*, 1997, **9**, 2004–2012.

[3] P. G. Lacroix, R. Clément, K. Nakatani, J. Zyss, and I. Ledoux, *Science*, 1994, **263**, 658–660.

[4] S. Bénard, A. Léaustic, E. Rivière, P. Yu, and R. Clément, *Chem. Mater.*, 2001, **13**, 3709–3716.

[5] S. Floquet, S. Salunke, M. L. Boillot, R. Clément, F. Varret, K. Boukheddaden, and E. Rivière, *Chem. Mater.*, 2002, **14**, 4164–4171.

[6] R. Brec, D. M. Schleich, G. Ouvrard, A. Louisy, and J. Rouxel, *Inorg. Chem.*, 1979, **18**, 1814–1818.

[7] I. Kerrache, C. Julien, and C. Sourisseau, *Solid State Ionics*, 1996, **92**, 37–43.

[8] P. Jeevanandam and S. Vasudevan, *Solid State Ionics*, 1997, **104**, 45–55.

[9] R. Clément, O. Garnier, and J. Jegoudez, *Inorg. Chem.*, 1986, **25**, 1404–1409.

[10] G. Ouvard, R. Brec, and J. Rouxel, *Mater. Res. Bull.*, 1985, **20**, 1181–1189.

[11] J. Qin, C. Yang, K. Yakushi, Y. Nakazawa, and K. Ichimura, *Solid State Commun.*, 1996, **100**, 427–431.

[12] R. Jakubiak and A. H. Francis, *J. Phys. Chem.*, 1996, **100**, 362–367.

[13] C. N. Field, M. L. Boillot, and R. Clément, *J. Mater. Chem.*, 1998, **8**, 283–284.

[14] S. J. Mason, S. J. Heyes, and D. O'Hare, *J. Chem. Soc., Chem. Commun.*, 1995, pp. 1657–1658.

[15] J. S. O. Evans, D. O'Hare, and R. Clément, *J. Am. Chem. Soc.*, 1995, **117**, 4595–4606.

[16] A. Leaustic, E. Riviere, R. Clément, E. Manova, and I. Mitov, *J. Phys. Chem.*, 1999, **B103**, 4833–4838.

[17] A. Léaustic, J. P. Audière, D. Cointereau, and R. Clément, *Chem. Mater.*, 1996, **8**, 1954–1961.

[18] H. Eckert, *NMR Basic Principles and Progress*, 1994, **33**, 125–198.

[19] X. Bourdon, A.-R. Grimmer, and V. P. Cajipe, *Chem. Mater.*, 1999, **11**, 2680–2686.

[20] J. Schmedt auf der Günne, S. Kaczmarek, L. van Wüllen, H. Eckert, D. Paschke, A. J. Foecker, and W. Jeitschko, *J. Solid State Chem.*, 1999, **147**, 341–349.

[21] M. Feike, R. Graf, I. Schnell, C. Jäger, and H. W. Spiess, *J. Am. Chem. Soc.*, 1996, **118**, 9631–9634.

[22] J. Schmedt auf der Günne and H. Eckert, *Chem. – Eur. J.*, 1998, **4**, 1762–1767.

[23] J. C. C. Chan and G. Brunklaus, *Chem. Phys. Lett.*, 2001, **349**, 104–112.

[24] W. Klingen, R. Ott, and H. Hahn, *Z. Anorg. Allg. Chem.*, 1973, **396**, 271–278.

[25] G. Courbion and G. Ferey, *J. Solid State Chem.*, 1988, **76**, 426–431.

[26] R. R. Ernst, G. Bodenhausen, and A. Wokaun, *Principles of nuclear magnetic resonance in one and two dimensions*, International Series of Monographs on Chemistry, Oxford University Press, 1987.

[27] Y. K. Lee, N. D. Kurur, M. Helmle, O. G. Johannessen, N. C. Nielsen, and M. H. Levitt, *Chem. Phys. Lett.*, 1995, **242**, 304–309.

[28] N. F. Ramsey, *Phys. Rev.*, 1959, **78**, 669.

[29] C. J. Jameson and H. S. Gutowsky, *J. Chem. Phys.*, 1964, **40**, 1714.

[30] G. Regelsky *Strukturelle Untersuchungen an kristallinen und glasigen Thio- und Selenophosphaten und ihren Schmelzen* PhD thesis, University of Münster, 2000.

List of Figures

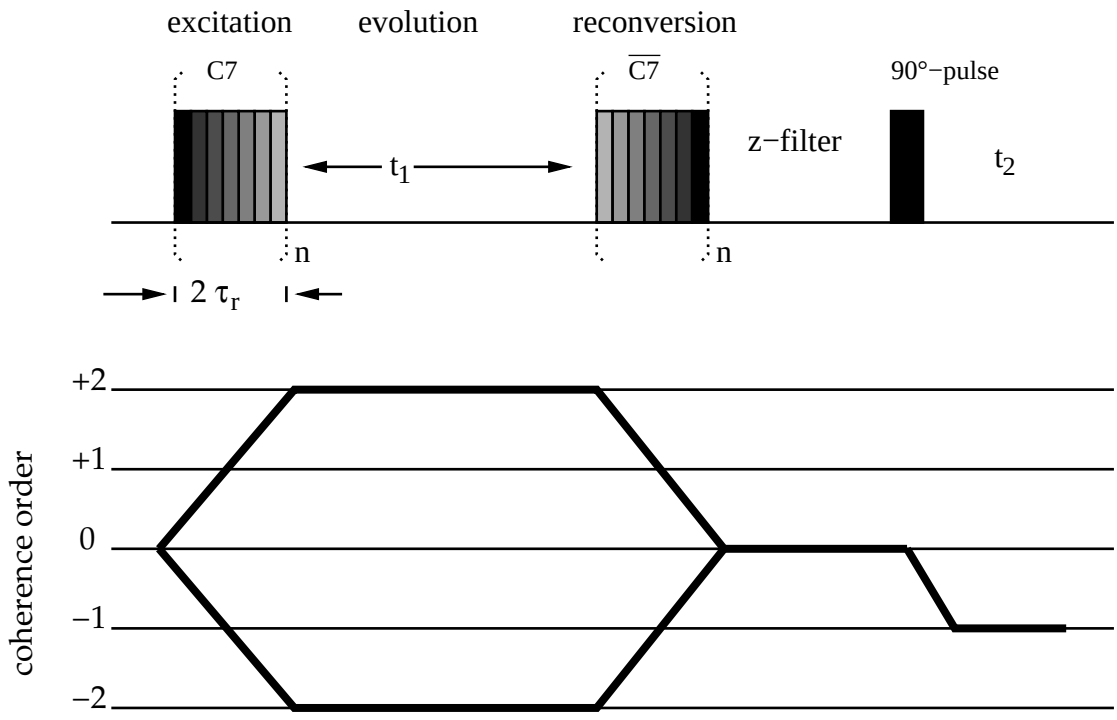

Figure 1: Schematic presentation of the pulse sequence used for the ^{31}P double-quantum experiments.

Table 1: Metal electronegativities (Pauling scale) and isotropic ^{31}P NMR chemical shifts of $P_2S_6^{2-}$ and PS_4^{3-} ions in crystalline metalthiophosphates [30]

Crystal	EN	δ_{iso}/ppm	Crystal	EN	δ_{iso}/ppm
$K_2P_2S_6$	0.82	32.6	$KTiPS_5$	0.82	77.1
$Li_2P_2S_6$	0.98	54.9	Li_3PS_4	0.98	88.4
$Ag_2P_2S_6$	1.93	64.4	Li_7PS_6	0.98	86.6
			Ag_3PS_4	1.93	103.0
			Ag_7PS_6	1.93	101.7
			$Ag_7P_3S_{11}$	1.93	103.3

Table 2: Estimate for the second interaction spot of methylviologen dependent on the first; A, B, C abbreviate probabilities of interaction spots of type A, B and C (see also figure 12); in the example in the text spot 1 is fixed as type C thus for spot 2 results a population probability of 37.5% which is higher than the random distribution value.

spot 2 $\rightarrow$ $\downarrow$ spot 1	A	B	C
A	25%	50%	25%
B	16.7%	50%	33.3%
C	12.5%	50%	37.5%

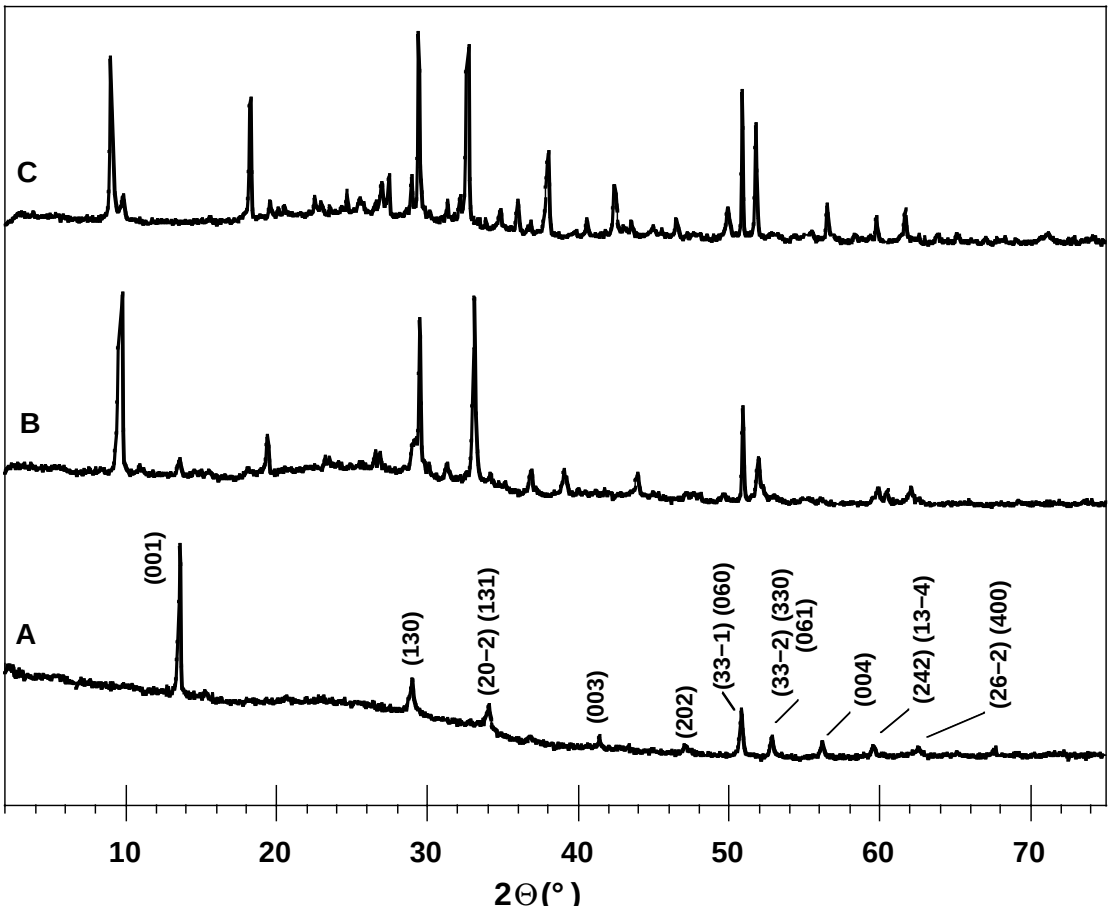

Figure 2: X-ray patterns recorded on A: pure $CdPS_3$, B: potassium intercalate and C: methylviologen intercalate.

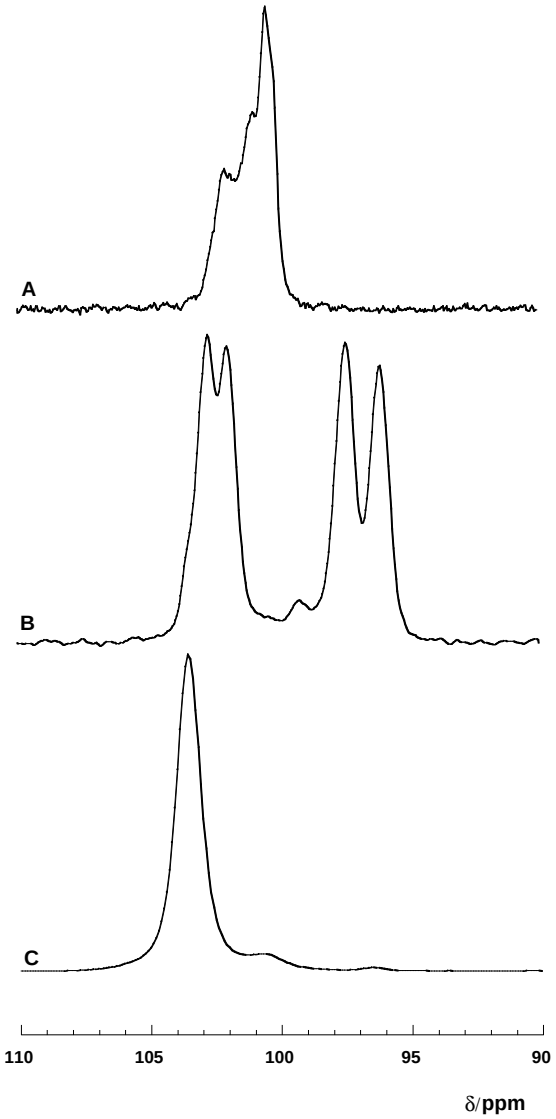

Figure 3: ^{31}P MAS NMR spectroscopy of A: Methylviologen intercalate, B: potassium intercalate, C: crystalline $CdPS_3$(peaks at 96.5 ppm and 100.5 ppm are due to impurities, presenting less than 4% of the overall intensity); spinning sidebands represent less than 5% of the total intensity.

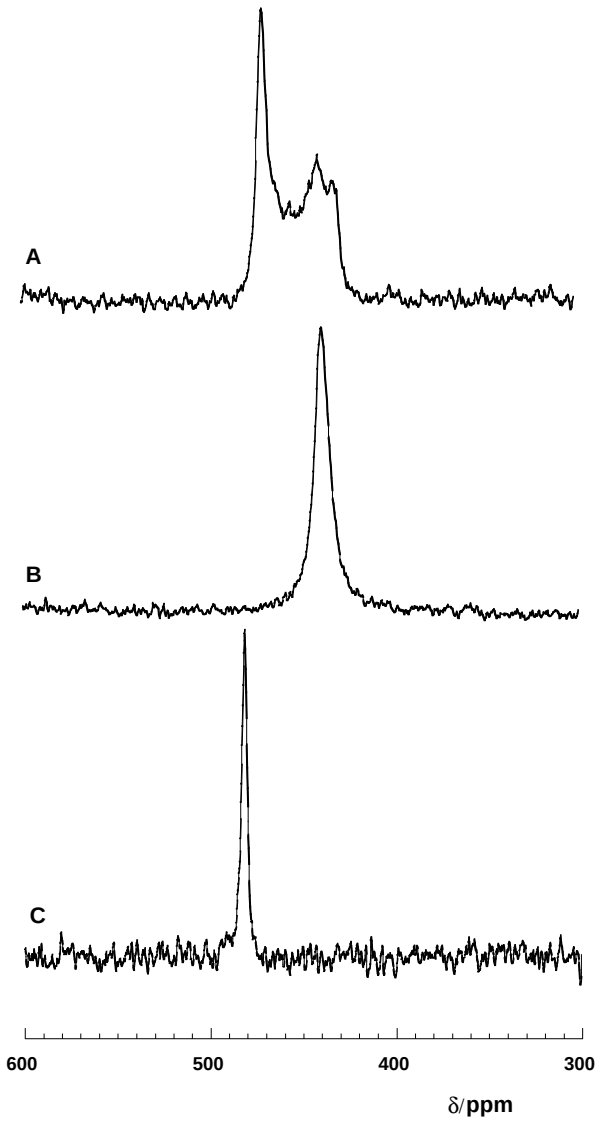

Figure 4: ^{113}Cd MAS NMR spectroscopy of A: Methylviologen intercalate, B: potassium intercalate, C: crystalline $CdPS_3$.

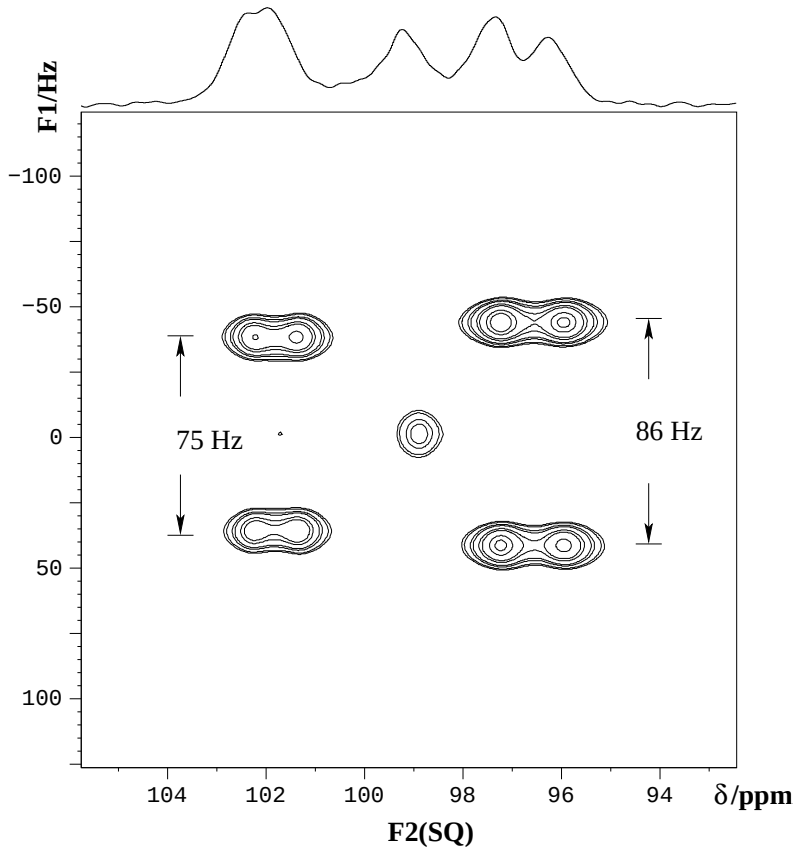

Figure 5: ^{31}P MAS 2D-spin echo NMR of potassium intercalated $CdPS_3$.

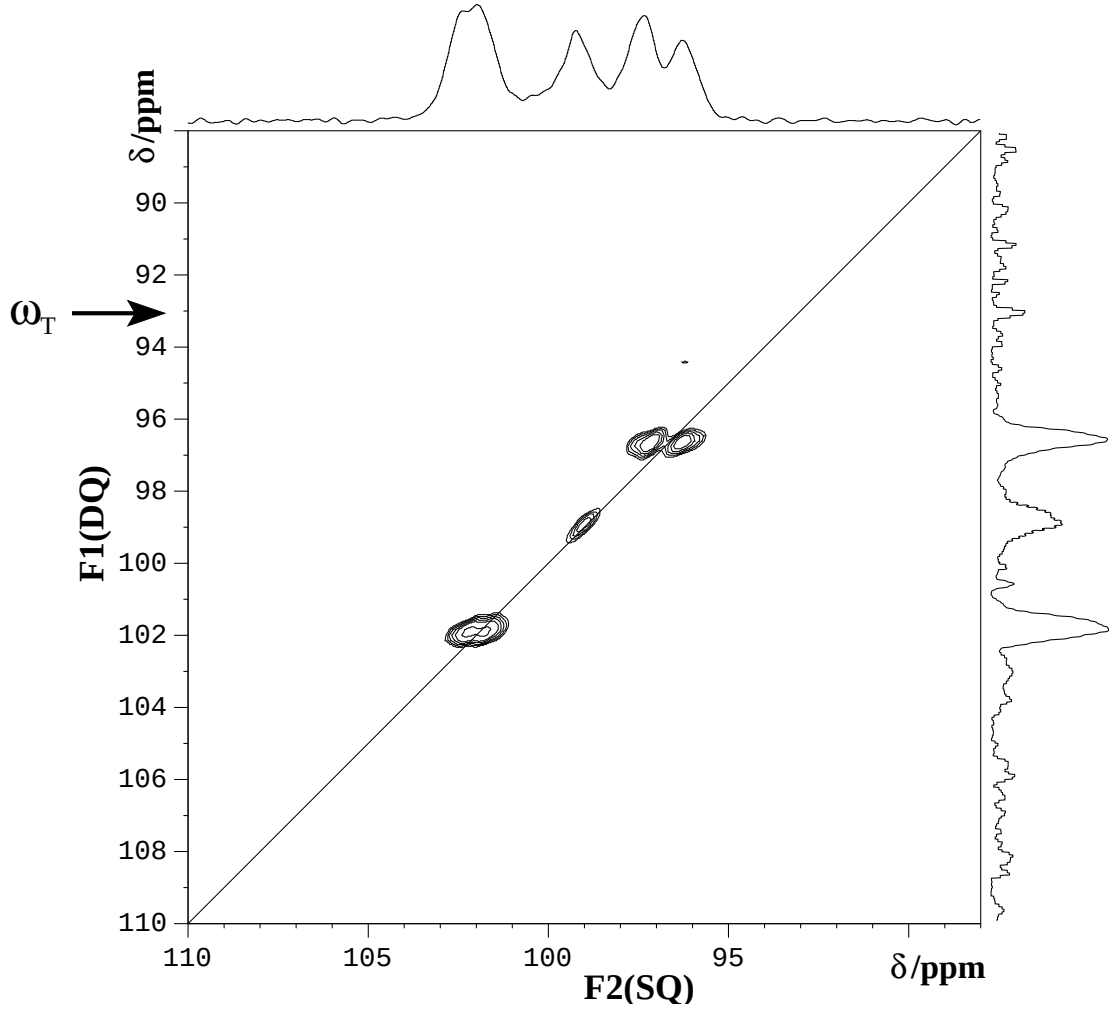

Figure 6: 2D ^{31}P MAS double-quantum spectrum of potassium intercalated $CdPS_3$, the transmitter frequency is denoted with ω_T.

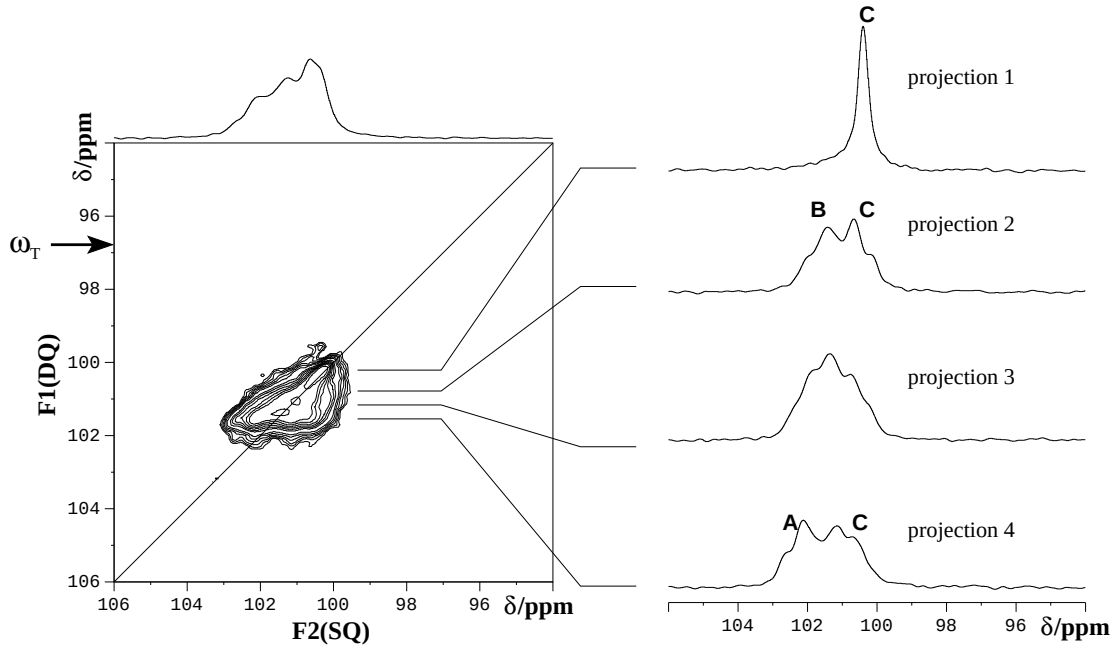

Figure 7: 2D ^{31}P MAS double-quantum spectrum of methylviologen intercalated $CdPS_3$, the transmitter frequency is denoted with ω_T; in the discussion three types of interaction spots A, B and C are defined, these can be assigned to the ^{31}P resonances in the cross sections.

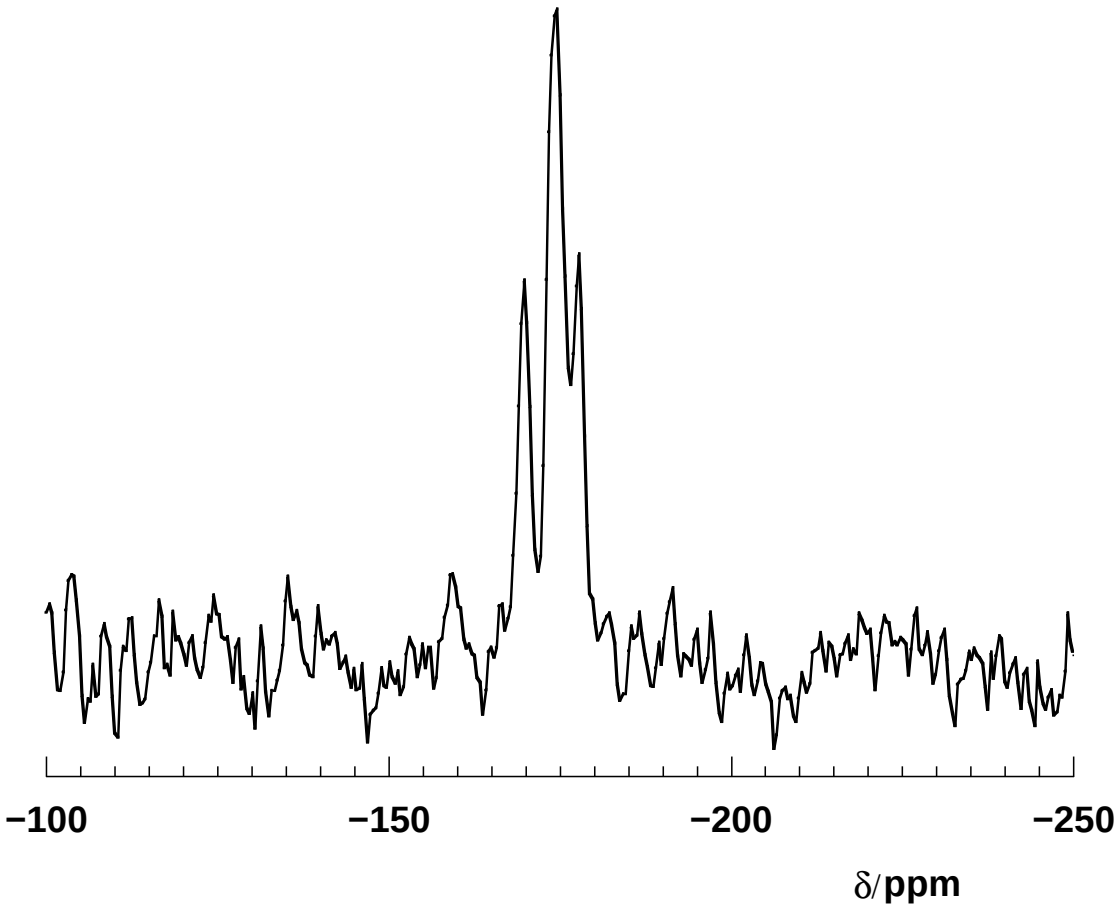

Figure 8: ^{15}N CP MAS NMR spectrum of methylviologen intercalated $CdPS_3$.

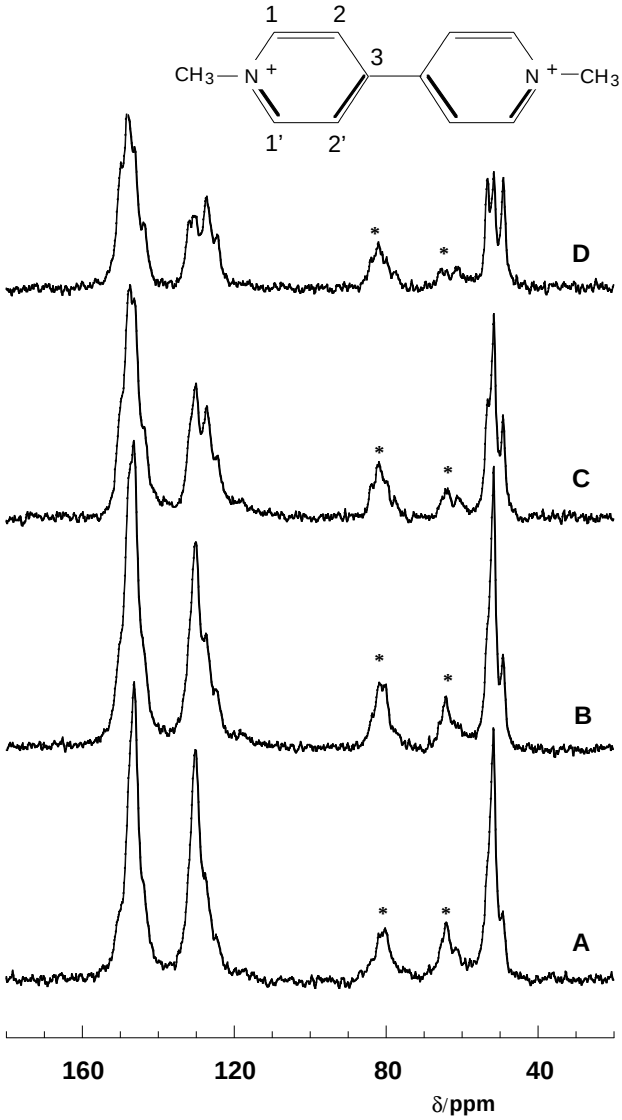

Figure 9: ^{13}C CP MAS NMR spectrum of methylviologen intercalated $CdPS_3$; contact time 100 μs (A), 1 ms (B), 5 ms (C), 10 ms (D); "*" denote spinning sidebands.

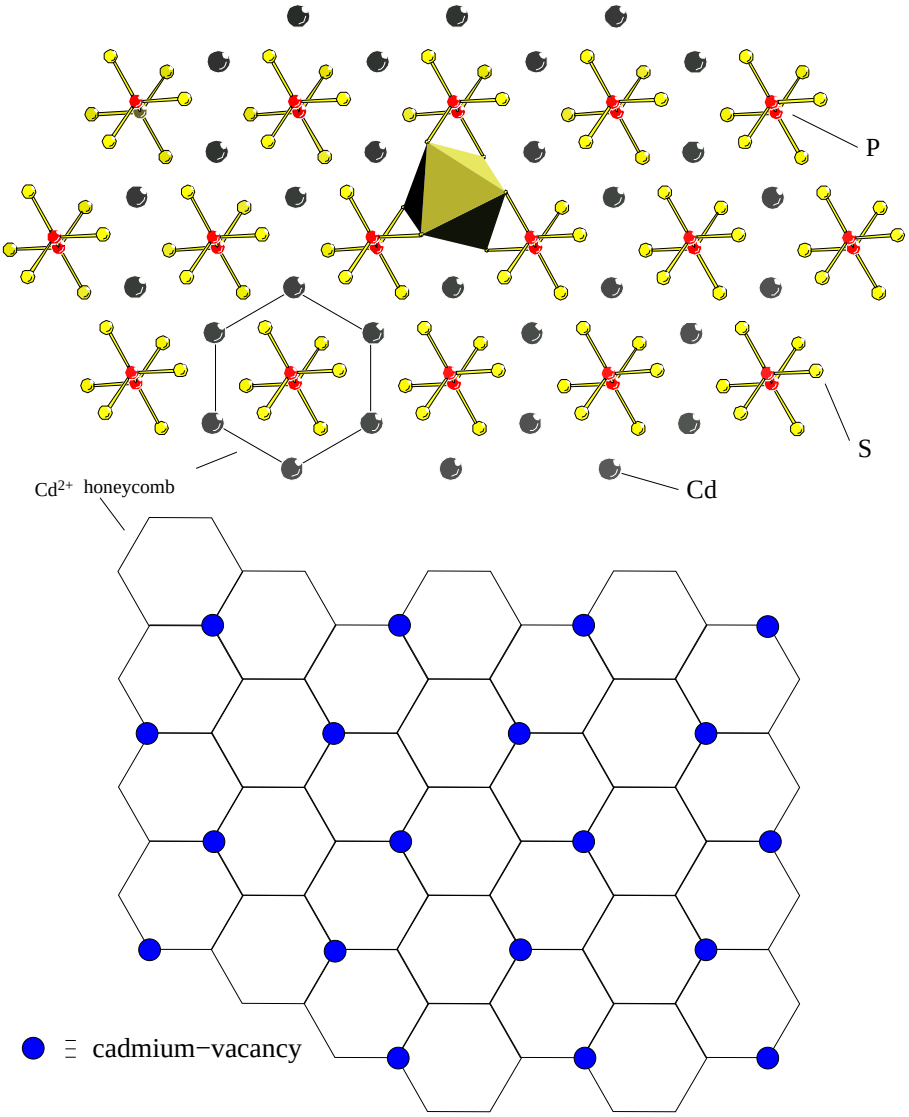

Figure 10: Cadmium vacancies in a $CdPS_3$-layer for a vacancy concentration of 1 in 4 cadmium sites with regard to pure $CdPS_3$.

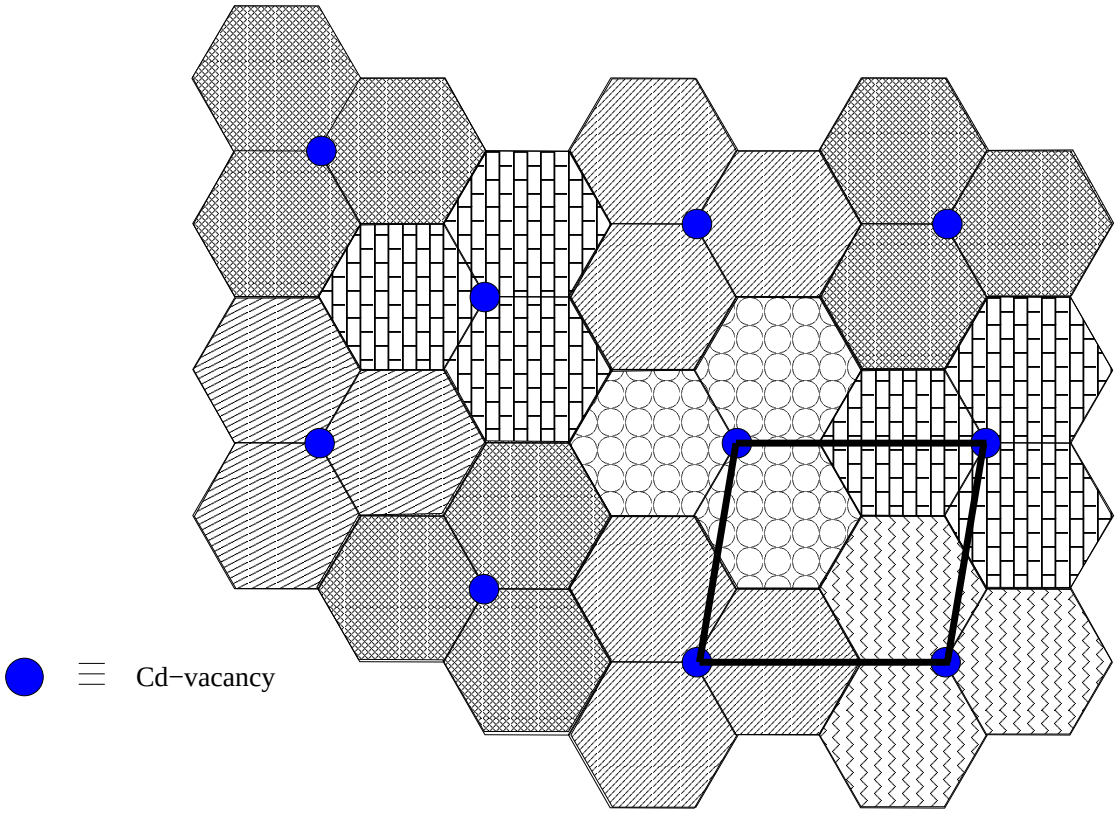

Figure 11: Cadmium vacancies in a $CdPS_3$-layer for a vacancy concentration of 1 in 6 with regard to pure $CdPS_3$; the trapezoid indicates a unit cell in case of perfect ordering in the layer.

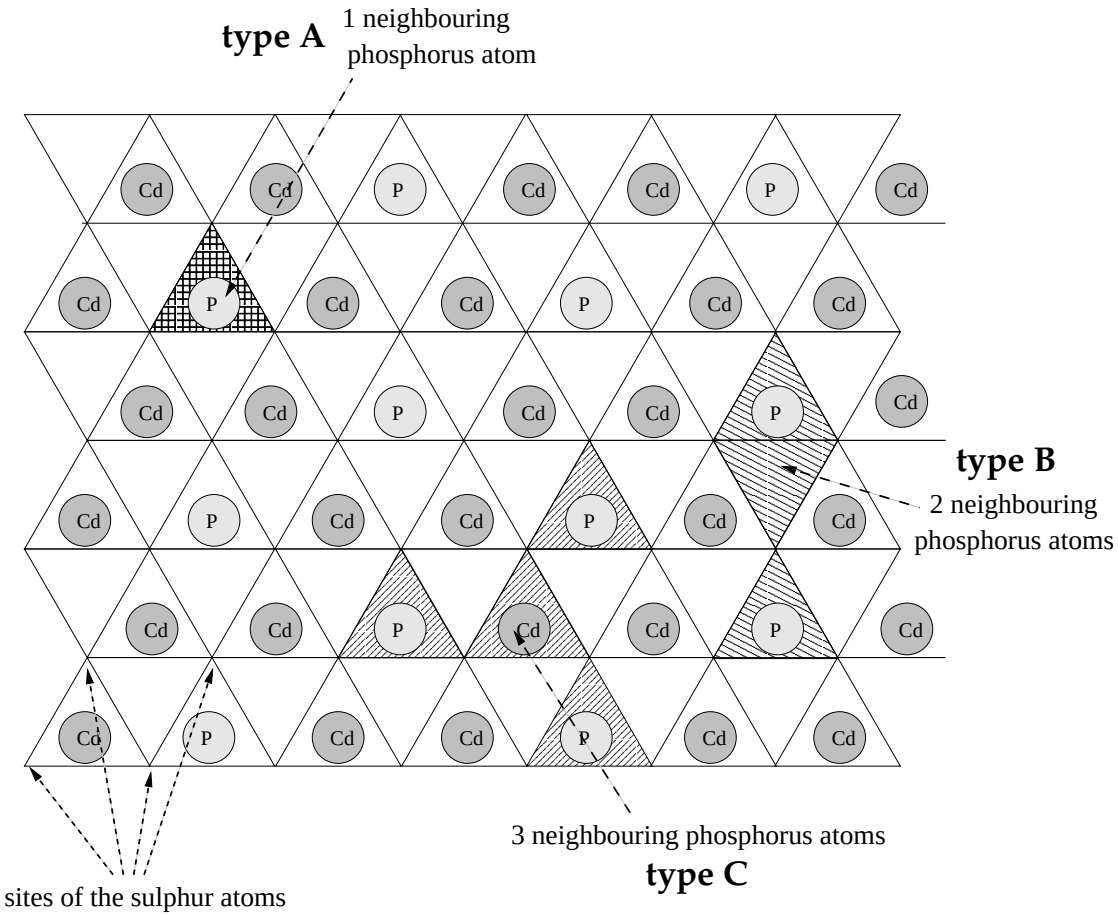

Figure 12: Interaction spots for the methylviologen dication; triangle structure is spanned by the sulphur atoms on one side of the layer; below the sulphur atoms sited are cadmium, phosphorus and vacancies; in dependence on these three possibilities it is possible to classify different types of triangles which are denoted type A, B and C in the figure.

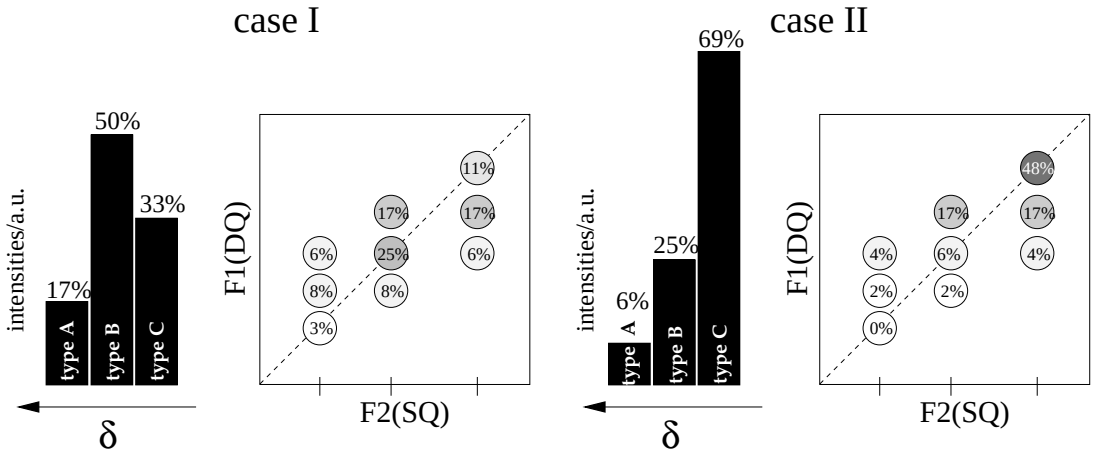

Figure 13: Schematic intensity distribution in the ^{31}P spectra for the different MV^{2+} distribution scenarios as described in the text; a description of the interaction spots A, B and C is given in figure 12.